

Diamagnetic Response of Metallic Photonic Crystals at Infrared and Visible Frequencies

Xinhua Hu,¹ C. T. Chan,² Jian Zi,³ Ming Li,¹ and Kai-Ming Ho¹

¹Ames Laboratory and Department of Physics and Astronomy, Iowa State University, Ames, Iowa 50011, USA

²Department of Physics, Hong Kong University of Science and Technology, Clear Water Bay, Kowloon, Hong Kong, China

³Surface Physics Laboratory (National Key Lab), Fudan University, Shanghai 200433, People's Republic of China

(Received 28 February 2006; published 5 June 2006)

We show analytically and numerically that diamagnetic response (effective magnetic permeability $\mu_e < 1$) at infrared and visible frequencies can be achieved in photonic crystals composed of metallic nanowires or nanospheres when the wavelength λ is much larger than the lattice constant a ($\lambda \sim 2000a$). When $\lambda \sim 100a$, the metallic photonic crystals will exhibit strong diamagnetic response ($\mu_e < 0.8$), leading to many interesting phenomena such as the unusual Brewster angle for s waves and incident-angle-and-polarization-independent reflection and transmission.

DOI: 10.1103/PhysRevLett.96.223901

PACS numbers: 42.70.Qs, 42.25.-p, 78.20.Ci

Photonic crystals (PCs) [1], or periodic composite media, have received great interest due to their unique electromagnetic (EM) properties. A famous example is the photonic band gaps (frequency ranges in which wave propagations are forbidden) which can be utilized to localize and guide light in a unique way [1,2]. Recently, the low-frequency range much below the first band gap has also attracted growing attention [3–6] due to the occurrence of PCs composed of (carbon) nanotubes [7] or (metallic [8] and semiconductor [9]) nanowires. In the long-wavelength limit (wavelength λ much larger than the lattice constant a), these PCs can be viewed as homogenous media described by an effective dielectric constant ϵ_e and an effective magnetic permeability μ_e [10]. Because of the diversity of microstructures and dielectric constant, ϵ_e of PCs can be tailored to be of strong anisotropy and of diverse values, resulting in many interesting phenomena that are difficult to be realized in natural crystals, e.g., Dyakonov surface waves [5] and ultraslow guided modes [6].

Conventional materials that exhibit magnetic response ($\mu \neq 1$) are far less common in nature than materials that exhibit electric response, and they are particularly rare at infrared (ir) and visible frequencies (common ferromagnetic and antiferromagnetic systems work at frequencies below 1 THz) [11,12]. Consequently, it is very difficult to achieve magnetic response in ir and visible ranges even with composite materials. Recently, Pendry *et al.* [13] proposed that split rings composed of nonmagnetic metal could exhibit strong magnetic response due to the inherent LC resonance and hence an effectively negative μ can be obtained at ir and visible frequencies ($\lambda \sim 10a$), leading to many novel concepts and potential applications as well [12–15]. However, it is generally believed that usual PCs should not exhibit magnetic response as magnetic resonances do not exist [3–6,10].

In this Letter, we study the long-wavelength behavior of metallic PCs (MPCs) consisting of metallic cylinders or spheres. Analytical formulas are derived for ϵ_e and μ_e within the coherent-potential approximation (CPA) [16,17] and their accuracy is confirmed by accurate multiple scat-

tering [Korringa-Kohn-Rostoker (KKR)] calculations [18,19]. We show that diamagnetic response ($\mu_e < 1$) at ir and visible frequencies can be achieved in the MPCs when the wavelength is still much longer than the unit-cell size ($\lambda \sim 2000a$ for the $a = 150$ nm case). When $\lambda \sim 100a$, MPCs will exhibit strong diamagnetic response ($\mu_e < 0.8$), leading to many interesting phenomena such as the unusual Brewster angle for s waves and incident-angle-and-polarization-independent reflection and transmission. We stress that the magnetic response of our MPCs is different from the metallic split-ring resonators (SRRs) since it does not rely on the magnetic resonances. Although the magnetic response of MPCs is weaker than that of SRRs, it can occur in a wider frequency range.

We first consider a 2D PC composed of circular cylinders of (ϵ_1, μ_1) and radius r in the matrix of (ϵ, μ) as shown in Fig. 1(a). For propagation of waves parallel to the plane of periodicity there exist two independent TE and TM modes (the H and E field is parallel to the cylinders, respectively). For TE modes, the magnetic field obeys

$$(\nabla^2 + k^2)H_z = 0, \quad (1)$$

which is subjected to the continuities of H_z and $\frac{1}{\epsilon} \partial H_z / \partial \rho$ at the surface of each cylinder (in the cylindrical coordinates (ρ, θ) with origin at the center of cylinder). The wave number in the cylinder and the matrix is given by $k_1 = \sqrt{\epsilon_1 \mu_1} k_0$ ($k_0 = \omega/c$, where ω is the angular frequency

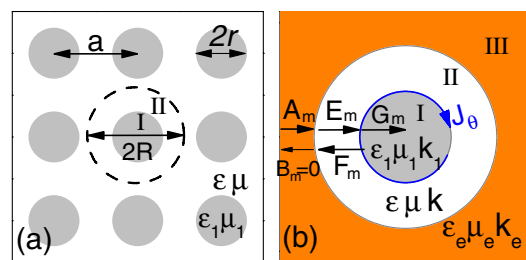


FIG. 1 (color online). (a) A 2D (3D) PC composed of cylinders (spheres) of (ϵ_1, μ_1) in the matrix of (ϵ, μ) , and (b) a coated cylinder (sphere) in the effective medium of (ϵ_e, μ_e) .

and c is the light speed in vacuum) and $k = \sqrt{\varepsilon}\sqrt{\mu}k_0$. In the following, we will focus on the TE mode and the results can be applied to TM mode simply by replacing (H_z, ε, μ) with (E_z, μ, ε) .

Then we derive analytical formulas for ε_e and μ_e with the CPA method [16,17] in the long-wavelength limit. We consider a ‘‘circular unit cell’’ (coated cylinder) of radius $R = S_u/\sqrt{\pi}$ (where S_u is the area of a unit cell; e.g., $S_u = a^2$ for square lattices. So the filling fraction $f_s = \frac{\pi r^2}{S_u} = \frac{r^2}{R^2}$)

$$\frac{\frac{1}{\varepsilon}kJ'_m(kR) - J_m(kR)\frac{1}{\varepsilon_e}k_eJ'_m(k_eR)/J_m(k_eR)}{\frac{1}{\varepsilon}kH'_m(kR) - H_m(kR)\frac{1}{\varepsilon_e}k_eJ'_m(k_eR)/J_m(k_eR)} = \frac{\frac{1}{\varepsilon}kJ'_m(kr) - J_m(kr)\frac{1}{\varepsilon_1}k_1J'_m(k_1r)/J_m(k_1r)}{\frac{1}{\varepsilon}kH'_m(kr) - H_m(kr)\frac{1}{\varepsilon_1}k_1J'_m(k_1r)/J_m(k_1r)}. \quad (2)$$

We note that the second term in Eq. (2) is just the m th-order scattering coefficient of the core cylinder [from which the first term can be obtained by replacing (r, k_1, ε_1) by (R, k_e, ε_e)]. If we only consider the scattering of cylindrical waves of the two lowest orders $m = 0$ and 1, ε_e and μ_e can be solved numerically from Eq. (2) [by changing Eq. (2) as $C_m = \frac{1}{\varepsilon_e}k_eJ'_m(k_eR)/J_m(k_eR)$].

When $ka, k_e a \ll 1$, Eq. (2) with $m = 0$ and 1 becomes

$$\mu_e = (1 - f_s)\mu + f_s\tilde{\mu}_1, \quad \frac{\varepsilon_e - \varepsilon}{\varepsilon_e + \varepsilon} = \frac{\tilde{\varepsilon}_1 - \varepsilon}{\tilde{\varepsilon}_1 + \varepsilon}f_s, \quad (3)$$

$$\tilde{\mu}_1 = \mu_1 p(k_1r), \quad p(x) = -2J'_0(x)/[xJ_0(x)], \quad (4)$$

$$\tilde{\varepsilon}_1 = \varepsilon_1 g(k_1r), \quad g(x) = J_1(x)/[xJ'_1(x)], \quad (5)$$

where $p(0) = g(0) = 1$, $p(x), g(x) \approx 1$ when $0 < |x| < 1$, $p(ix) \approx 2/x$, and $g(ix) \approx 1/x$ when $x > 2$ [20].

For conventional dielectric PCs with comparable ε_1 and ε , $k_1r \ll 1$ when $ka \ll 1$ and Eqs. (3)–(5) always reduce to the Maxwell-Garnett (MG) formulas (by $\tilde{\mu}_1 = \mu_1$ and $\tilde{\varepsilon}_1 = \varepsilon_1$) [10], namely

$$\mu_e = (1 - f_s)\mu + f_s\mu_1, \quad \frac{\varepsilon_e - \varepsilon}{\varepsilon_e + \varepsilon} = \frac{\varepsilon_1 - \varepsilon}{\varepsilon_1 + \varepsilon}f_s. \quad (6)$$

But in MPCs, $k_1r \ll 1$ only when $ka \rightarrow 0$ [$\varepsilon_1 = 1 - f_p^2/(f^2 + if_\tau f) \approx if_p^2/f_\tau f$ when $f \rightarrow 0$]. When ka is not so small ($\varepsilon_1 \approx -f_p^2/f^2$), $k_1r \approx ir/\delta_p$, where $\delta_p = c/2\pi f_p$ is the skin depth of metal (~ 13 nm for Al) in the ir or visible range. $\tilde{\mu}_1 \approx \mu_1$ and the MG formulas will be valid only when $r < \delta_p$. When $r > \delta_p$, $\tilde{\mu}_1 < \mu_1$ and MPCs will be effectively diamagnetic. Especially when $r > 40\delta_p$ and $\lambda < 100a$ (to be shown later), $\tilde{\mu}_1 \approx 0$ and the MPCs will exhibit strong diamagnetic response.

There exists a particular case of perfect metallic PCs (PMPCs) [3]. Using $\mu_1 = 1$ and $\varepsilon_1 = -f_p^2/f^2$ ($f_p \rightarrow +\infty$), Equations (3)–(5) become (by $\tilde{\mu}_1 = 0$ and $\tilde{\varepsilon}_1 = -\infty$):

$$\mu_e = (1 - f_s)\mu, \quad \varepsilon_e = \varepsilon(1 + f_s)/(1 - f_s). \quad (7)$$

Equation (7) can also be derived using the CPA method and the boundary condition of $\partial H_z^I(r)/\partial \rho = 0$ (TE) for perfect-metal cylinders [17]. Previously, Nicorovici *et al.* [3] found an interesting problem in PMPCs of $\varepsilon = \mu = 1$ that the refraction index $n_e = \sqrt{1 + f_s}$ could not be ex-

plained using the MG theory and $\varepsilon_1 = -\infty$. Now the problem is clear that $n_e = \sqrt{\varepsilon_e}\sqrt{\mu_e}$ and Eq. (7) should be used for PMPCs, agreeing with the recent suggestion by Krokhin and Reyes [3].

To check the validity of the above analytic formulas, we use the S -matrix-combined KKR method (including high-order cylindrical waves) [18,19] and do the transmission calculations for the normal incidence of a plane wave upon a MPC slab. Then the ε_e and μ_e of MPCs can be obtained from the complex transmission and reflection coefficients [14,21]. In Fig. 2, we show the accurate KKR results of ε_e and μ_e for a square lattice of Al cylinders in air with $a = 150$ nm and $r = 52.5$ nm together with those from different formulas. It can be seen that the MG formulas are only valid when $\lambda > 2000a$ and the MPCs are nonmagnetic. For higher frequencies, the MPCs become effectively diamagnetic and Eqs. (3)–(5) (when $120a < \lambda < 2000a$) or direct solution of Eq. (2) (when $5a < \lambda < 120a$) should be used.

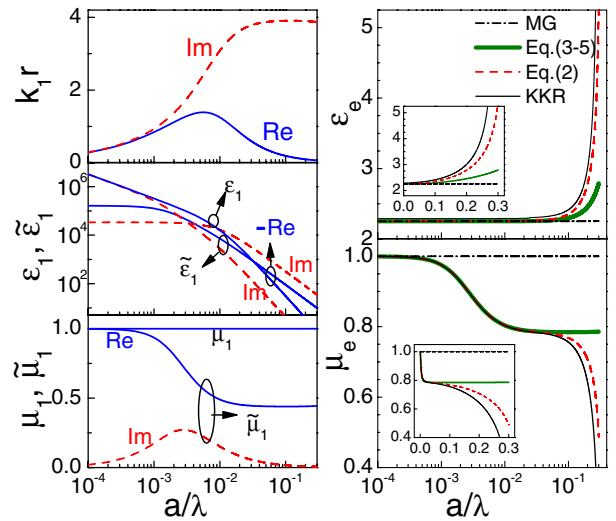


FIG. 2 (color online). k_1r , ε_1 , $\tilde{\varepsilon}_1$, μ_1 , $\tilde{\mu}_1$, ε_e (real part), and μ_e (real part) of a 2D PC (square lattice) of aluminum cylinders in air in the lowest TE band [$0 < \text{Im}(\varepsilon_e) < 0.04$, $0 < \text{Im}(\mu_e) < 0.09$]. The lattice constant $a = 150$ nm and the radius of cylinder $r = 52.5$ nm. $\mu_1 = 1$ and a Drude model of $\varepsilon_1 = 1 - f_p^2/(f^2 + if_\tau f)$ are used for Al where $f_p = 3570$ THz, $f_\tau = 19.4$ THz.

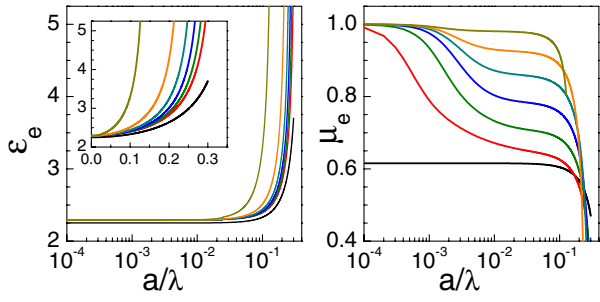


FIG. 3 (color online). KKR results of ε_e and μ_e of 2D PCs (square lattice) of Al (from top to bottom: the lattice constant $a = 25, 55, 90, 150, 300, 1000$ nm) or perfect-metal (the bottom line) cylinders ($r/a = 0.35$) in air for TE mode.

The MPC will be strongly effectively diamagnetic ($\mu_e < 0.8$) when $\lambda < 100a$. When $\lambda < 120a$ (approaching the band gap), μ_e will decrease strongly and diverge at the band edge due to the Bragg resonance. At high frequencies near the band gap ($\lambda < 5a$), the scattering of high-order cylindrical waves will be important and more accurate KKR calculations are needed.

In Fig. 3, we show the KKR results of ε_e and μ_e for square lattices of Al and perfect-metal cylinders ($r/a = 0.35$) in air. It can be seen that the MPCs have almost the same $\varepsilon_e \approx 2.28$ when $\lambda > 50a$. But μ_e will be quite different for MPCs with varying the lattice constant a . When $\lambda > 10a$, the MPC with $a < 25$ nm (so $r < 0.7\delta_p$) behaves nonmagnetically and those with larger a can be effectively diamagnetic. When $a > 1.5 \mu\text{m}$ (so $r > 40\delta_p$), the MPC can have almost the same diamagnetic property with PMPC for $\lambda < 100a$.

The ε_e and μ_e of MPCs can be used to determine the optical properties of MPCs, such as refraction, reflection, and transmission [11]. Here we will focus on the Brewster angle (θ_b) phenomenon, i.e., total transmission of TE waves at a particular incident angle θ_b . In usual dielectric materials, the zero reflection occurs when the reflected rays are perpendicular to the refracted rays due to the zero EM emission of electric dipoles (excited by refracted waves) in the dipolar direction. But for the MPCs with $\mu_e < 1$, magnetic dipoles will also be excited and this perpendicularity does not exist. It can be shown that

$$\theta_b = \arctan \sqrt{(\mu_b \varepsilon_e^2 - \varepsilon_b \varepsilon_e \mu_e) / (\varepsilon_b \varepsilon_e \mu_e - \mu_b \varepsilon_b^2)} \quad (8)$$

for a MPC in the background with ε_b and μ_b [11]. In Fig. 4, we show the Brewster angle for a square lattice of

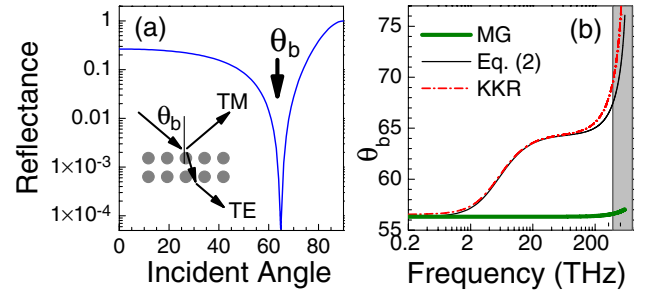


FIG. 4 (color online). (a) Reflectance as a function of the incident angle θ at $\lambda = 1550$ nm (TE incidence), and (b) Brewster angle as a function of the frequency of incident waves for a two layer of the 2D MPC studied in Fig. 2 (the transmittance is less than 5×10^{-9} for the TM incidence). The light shaded range stands for the visible frequencies.

Al cylinders in air ($a = 150$ nm, $r = 52.5$ nm). The θ_b predicted by Eqs. (2) and (8) agrees well with the accurate KKR value. For frequencies lower than 1 THz, the MPC will be nonmagnetic ($\varepsilon_e = 2.28$, $\mu_e \approx 1$) and $\theta_b \approx 56.5^\circ$. When $f = 193$ THz ($\lambda = 1550$ nm), the MPC will exhibit strong diamagnetic response and $\theta_b = 65.5^\circ$. Previously, 2D MPCs can act as ir polarizers (usually working at normal incidence) due to the low-frequency band gap for TM waves. Our results indicate that 2D MPCs can further act as ir TE-TM splitters at θ_b . We note that this complete splitting of TE and TM waves does not exist at dielectric interfaces.

By now, we have shown the effectively diamagnetic behavior of 2D MPCs for the TE waves. This diamagnetic response can be understood by $\mu_e \equiv \langle B_z \rangle / \mu_0 \langle H_z \rangle = (1 - f_s) \mu + f_s \mu_1 \langle H_z^I \rangle / H_z^{II}$, where $\langle H_z \rangle = H_z^{II}$ ($\langle B_z \rangle = (1 - f_s) B_z^{II} + f_s \langle B_z^I \rangle$) is the average of H (B) field over the line-boundary (surface) of the unit cell [14]. For $m = 0$, $H_z^I = J_0(k_1 \rho)$, $H_z^{II} = H_z^I(r) = J_0(k_1 r)$ (when $ka \ll 1$), $\langle H_z^I \rangle \equiv 2r^{-2} \int_0^r H_z^I \rho d\rho = -2J_0'(k_1 r) / k_1 r$, and thus the μ_e in Eq. (3) can be alternatively obtained. We note that surface currents $J_\theta = (\varepsilon_1^{-1} - 1) [\nabla \times \mathbf{H}^I]_\theta \approx -\partial H_z^I / \partial \rho$ can be induced in metal cylinders [see Fig. 1(b)] and $\langle H_z^I \rangle = -2J_0'(k_1 r) / k_1 r$ can also be obtained by $\langle H_z^I \rangle = (\text{external}) H_z^{II} + (\text{induced}) r^{-2} \int_0^r J_\theta \rho^2 d\rho$. Since H_z^I decays inside the metallic cylinders and $\langle H_z^I \rangle < H_z^{II}$, μ_e can be less than 1 in MPCs.

Similar effective diamagnetic response can also exist in 3D MPCs consisting of metallic spheres. Unlike 2D, 3D MPCs can have isotropic μ_e and ε_e due to degenerated TE and TM modes at the low frequencies. Using similar CPA derivations, we can obtain the following relation

$$\frac{\frac{1}{\mu} \frac{\partial}{\partial R} [R j_l(kR)] - j_l(kR) \frac{1}{\mu_e} \frac{\partial}{\partial R} [R j_l(k_e R)] / j_l(k_e R)}{\frac{1}{\mu} \frac{\partial}{\partial R} [R h_l(kR)] - h_l(kR) \frac{1}{\mu_e} \frac{\partial}{\partial R} [R j_l(k_e R)] / j_l(k_e R)} = \frac{\frac{1}{\mu} \frac{\partial}{\partial r} [r j_l(kr)] - j_l(kr) \frac{1}{\mu_1} \frac{\partial}{\partial r} [r j_l(k_1 r)] / j_l(k_1 r)}{\frac{1}{\mu} \frac{\partial}{\partial r} [r h_l(kr)] - h_l(kr) \frac{1}{\mu_1} \frac{\partial}{\partial r} [r j_l(k_1 r)] / j_l(k_1 r)} \quad (9)$$

and another equation with replacing μ by ε from the zero H and E scattering [22], where j_l (h_l) is the l th spherical Bessel (Hankel) function. When ka , $k_e a \ll 1$, the equations with $l = 1$ (the lowest order in 3D) become

$$\frac{\mu_e - \mu}{\mu_e + 2\mu} = f_s \frac{\tilde{\mu}_1 - \mu}{\tilde{\mu}_1 + 2\mu}, \quad \frac{\varepsilon_e - \varepsilon}{\varepsilon_e + 2\varepsilon} = f_s \frac{\tilde{\varepsilon}_1 - \varepsilon}{\tilde{\varepsilon}_1 + 2\varepsilon}, \quad (10)$$

$$\tilde{\mu}_1 = \mu_1 q(k_1 r), \quad \tilde{\varepsilon}_1 = \varepsilon_1 q(k_1 r), \quad (11)$$

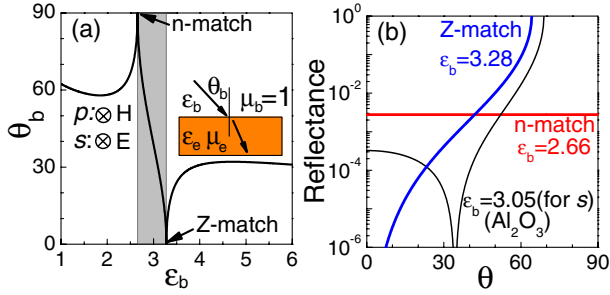


FIG. 5 (color online). (a) Brewster angle as a function of ϵ_b (the light gray area is for s waves and others for p waves), and (b) reflectance as a function of incident angle θ for the incidence of light at $\lambda = 1550$ nm from a dielectric media of ϵ_b to a 3D MPC of $\epsilon_e = 2.95$ and $\mu_e = 0.90$.

$$q(x) = 2/[1 + xj_1'(x)/j_1(x)], \quad (12)$$

where f_s is the volume ratio of spheres in PCs [15,20]. Since $q(x)$ behaves like $p(x)$, similar diamagnetic response (like Fig. 3) can occur in 3D MPCs in the long-wavelength limit.

It is known that the Brewster angle exists only for p waves at usual dielectric interfaces. However, at the interface between a dielectric medium of ϵ_b and a 3D MPC of ϵ_e and μ_e ($\mu_e < 1$), the Brewster angle can also exist for s waves when $\epsilon_e \mu_e < \epsilon_b < \epsilon_e / \mu_e$ (for p waves when $\epsilon_b < \epsilon_e \mu_e$ or $\epsilon_b > \epsilon_e / \mu_e$) [11]. For example, a simple-cubic lattice ($a = 150$ nm) of Al spheres of $r = 48.5$ nm in glass ($\epsilon = 2$) will be of $\mu_e = 0.90$ and $\epsilon_e = 2.95$ at $\lambda = 1550$ nm. When $2.66 < \epsilon_b < 3.28$, a Brewster angle exists for s waves (see Fig. 5); e.g., $\theta_b = 34.4^\circ$ for $\epsilon_b = 3.05$ (Al_2O_3). When $\epsilon_b = \epsilon_e / \mu_e = 3.28$ (impedance match), $\theta_b = 0^\circ$ and both s and p waves can totally enter the 3D MPC at normal incidence.

The reflection and transmission depend on both the incident angle and polarizations at dielectric interfaces. But at the interface between a dielectric medium of ϵ_b and a 3D MPC of ϵ_e and μ_e , the dependence will not exist when the refractive indices are matched, namely $\epsilon_b = \epsilon_e \mu_e$ [see Fig. 5(b), where the reflectance can be increased using a 3D MPC of larger f_s]. This interesting feature may facilitate the fabrication of some incident-angle-and-polarization-independent optical devices [23].

In summary, we have demonstrated effective diamagnetic response of MPCs in the very long-wavelength range ($\lambda < 2000a$) by nontrivial modifications of the Maxwell-Garnett formulas, leading to many interesting phenomena such as the unusual Brewster angle for s waves and incident-angle-and-polarization-independent reflection and transmission.

X.H. thanks Dr. N.A. Nicorovici for discussions on the lattice sums in Refs. [18,19] and providing an erratum of Ref. [18]. We also thank Dr. Zhao-Qing Zhang, Dr. Hongqiang Li, and Dr. Jensen Li for helpful discussions. This work is supported by the Director for Energy Research, Office of Basic Energy Sciences. J.Z. acknowl-

edges support from CNKBRF and NSFC. The Ames Laboratory is operated for the U. S. Department of Energy by Iowa State University under Contract No. W-7405-ENG-82.

- [1] E. Yablonovitch, Phys. Rev. Lett. **58**, 2059 (1987); S. John, Phys. Rev. Lett. **58**, 2486 (1987).
- [2] K. Sakoda, *Optical Properties of Photonic Crystals* (Springer, Berlin, 2001).
- [3] N.A. Nicorovici, R.C. McPhedran, and L.C. Botten, Phys. Rev. Lett. **75**, 1507 (1995); A.A. Krokhin and E. Reyes, Phys. Rev. Lett. **93**, 023904 (2004).
- [4] F.J. Garcia-Vidal, J.M. Pitarke, and J.B. Pendry, Phys. Rev. Lett. **78**, 4289 (1997).
- [5] P. Halevi, A.A. Krokhin, and J. Arriaga, Phys. Rev. Lett. **82**, 719 (1999); D. Artigas and L. Torner, Phys. Rev. Lett. **94**, 013901 (2005).
- [6] J.T. Shen, P.B. Catrysse, and S. Fan, Phys. Rev. Lett. **94**, 197401 (2005).
- [7] S. Iijima, Nature (London) **354**, 56 (1991); K. Jiang, Q. Li, and S. Fan, Nature (London) **419**, 801 (2002).
- [8] B.H. Hong *et al.*, Science **294**, 348 (2001); G. Sauer *et al.*, J. Appl. Phys. **91**, 3243 (2002); Y.T. Pang *et al.*, Nanotechnology **14**, 20 (2003); X. Hu and C.T. Chan, Appl. Phys. Lett. **85**, 1520 (2004); X. Ao and S. He, Appl. Phys. Lett. **87**, 101112 (2005).
- [9] M.H. Huang *et al.*, Science **292**, 1897 (2001).
- [10] J.C. Maxwell Garnett, Philos. Trans. R. Soc. London **203**, 385 (1904); *Electrical Transport and Optical Properties of Inhomogeneous Media*, edited by J.C. Garland and D.B. Tanner (AIP, New York, 1978); D.E. Aspnes, Am. J. Phys. **50**, 704 (1982).
- [11] L.D. Landau and E.M. Lifshitz, *Electrodynamics of Continuous Media* (Pergamon Press, Oxford, 1984).
- [12] T.J. Yen *et al.*, Science **303**, 1494 (2004).
- [13] J.B. Pendry *et al.*, IEEE Trans. Microwave Theory Tech. **47**, 2075 (1999); R.A. Shelby *et al.*, Science **292**, 77 (2001); S. Linden *et al.*, Science **306**, 1351 (2004); J. Zhou *et al.*, Phys. Rev. Lett. **95**, 223902 (2005).
- [14] S. O'Brien and J.B. Pendry, J. Phys. Condens. Matter **14**, 4035 (2002).
- [15] A.K. Sarychev, R.C. McPhedran, and V.M. Shalaev, Phys. Rev. B **62**, 8531 (2000).
- [16] P. Sheng, *Introduction to Wave Scattering, Localization, and Mesoscopic Phenomena* (Academic Press, New York, 1995).
- [17] X. Hu and C.T. Chan, Phys. Rev. Lett. **95**, 154501 (2005).
- [18] L.C. Botten *et al.*, Phys. Rev. E **64**, 046603 (2001); L.C. Botten *et al.*, J. Opt. Soc. Am. A **17**, 2165 (2000).
- [19] V. Twersky, Arch. Ration. Mech. Anal. **8**, 323 (1961).
- [20] When $x \rightarrow 0$, $J_0(x) = 1$, $J_0'(x) = -J_1(x) = -\frac{x}{2}$, $J_1'(x) = \frac{1}{2}$, $H_0(x) = \frac{2i}{\pi} \ln(\frac{x}{2})$, $H_0'(x) = -H_1(x) = \frac{2i}{\pi x}$, $H_1'(x) = \frac{2i}{\pi x^2}$, $J_1(x) = \frac{x}{2}$, $J_1'(x) = \frac{1}{2}$, $h_1(x) = -\frac{i}{x^2}$, $h_1'(x) = \frac{2i}{x^3}$.
- [21] X. Hu, C.T. Chan, and J. Zi, Phys. Rev. E **71**, 055601(R) (2005).
- [22] N. Stefanou, V. Yannopoulos, and A. Modinos, Comput. Phys. Commun. **113**, 49 (1998).
- [23] E. Lidorikis *et al.*, Phys. Rev. Lett. **91**, 023902 (2003).